ebg MedAustron
2700 Wiener Neustadt – Austria

DOCUMENT ID	REV. NO.	STATUS
TN-111001-a-MVE	0.0	DRAFT

Date: 2011-10-05

Technical Note

High-Performance Digital Control of Magnet Power Supplies

PREPARED BY:	CHECKED BY:	APPROVED BY:
M. Veenstra	A. Beuret I. de Cesaris P. Fraboulet	

APPROVAL GROUP:

HISTORY OF CHANGES

REV. NO.	DATE	PAGES	DESCRIPTIONS OF THE CHANGES
0.0	2011-10-01	all	Draft version

TABLE OF CONTENTS

1 Introduction

In particle accelerators, magnetic fields must be produced in rapid cycles and controlled with a very high precision, which is typically in the range of 10^{-4} to 10^{-6}. Power supplies for these applications are realised with power-electronic converters of various types and sizes. They are mainly characterised by their power, which limits the attainable field energy and cycle rate, and their switching frequency, which limits the attainable control speed. Line-commutated converters equipped with thyristors—usually employed for high-current applications—have a relatively low switching frequency of several hundred hertz. Hard-switching converters equipped with IGBT or IGCT—used for low-, medium- and increasingly for high-power applications—can attain switching frequencies of several kilohertz, or even a few ten kilohertz at lower powers. Soft-switching converters equipped with MOSFET or IGBT—mainly used for low- and medium-power applications—can attain switching frequencies of several ten up to a hundred kilohertz.

To obtain rapid cycling with very high precision, a dedicated controller is needed for the magnet current or field[1]. This controller must track the reference function and reject any load perturbations with high bandwidth, while being sufficiently robust to variations in the system's parameters. Numerous control methods are available in the literature, such as [1–5]. Two main classes of controllers exist: those operating in the analogue domain and those operating in the digital domain.

Analogue controllers—mainly used for control of magnet power supplies at CERN until recently—have the advantage of simpler analysis and synthesis, but are limited to rather simple structures such as PID-controllers with only few degrees of freedom for tuning. Also, analogue electronics offer little flexibility once manufactured.

Digital controllers offer a vast design flexibility, at the cost of some particular phenomena inherent to sampled-data systems and somewhat lesser-known theory. Although the same control structures as with analogue controllers can be used, the control performance can significantly be improved using sophisticated digital control methods.

One of these methods is the so-called RST-controller with its synthesis [2–4]. It allows independent design of reference tracking and perturbation rejection. The synthesis is algebraic and is particularly well-suited for programming in digital computers. Figure 1 shows a digital RST-control loop of an analogue process (including signal conversions between the continuous- and discrete-time domains).

At CERN, digital RST-controllers have first been applied to control the currents of the Large Hadron Collider's (LHC) superconducting magnets [6]. In this particular application, the controller design is simple, because the bandwidth of the power supplies is three orders of magnitude bigger and the inverted time constant of the magnets three orders of magnitude smaller than the bandwidth of the controllers. In the following, RST-control has been applied to different medium- and high-power converters, where the bandwidths of the power supplies and loads are separated by at most one order of magnitude from those of the controllers. The applications include various converters of the Ions-for-LHC (I-LHC) project—a dozen converters for the Low-Energy Ion Ring (LEIR) and the Transfer Tunnel number 2 (TT2)—, the Proton-Synchrotron Booster (PSB) main power supply, and the Proton Synchrotron (PS) main power supplies—the old Main Power Supply (MPS) and the new Power for the PS (POPS).

This document describes the main issues in digital control in general, and those in application and design of RST-controllers for magnet power supplies in particular.

2 Sampling and Reconstruction

Sampled-data systems, such as computer-controlled systems or power converters, contain both continuous-time and discrete-time signals. The mixture of different signal types requires signal conversion from continuous to discrete time (sampling) and vice versa (reconstruction) [2–5]. These conversions cause some signal distortion, of which aliasing or frequency folding is the most peculiar effect.

Periodic sampling of a continuous-time signal $u(t)$ at the sampling instants kT, with T the sampling period and $k \in \mathbb{Z}$, results in the discrete-time signal $u(kT)$. The discrete-time signal's frequency spectrum $U^*(\omega)$ is the sum of

[1] Ideally, the magnet field is controlled directly instead of indirectly via its current. But a high-quality measurement of the latter is easier to realise than one of the former, especially in presence of a particle beam.

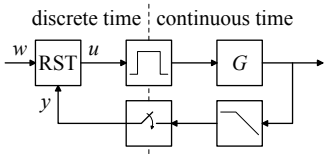

Figure 1: Digital RST-control loop of an analogue process.

the continuous-time signal's spectrum $U(\omega)$ and its displacements [2, 3, 7]

$$U^*(\omega) = \frac{1}{T} \sum_{k=-\infty}^{\infty} U(\omega + k\frac{2\pi}{T}). \tag{1}$$

Sampling causes copies of the original signal to be added to the frequency spectrum, a phenomenon known as aliasing or frequency folding. After sampling, it is no longer possible to distinguish the contributions from the frequencies $\omega + k\frac{2\pi}{T}$, with $k \in \mathbb{Z}$, and the frequency ω becomes the alias of these frequencies. Considering absolute values of frequencies, the baseband $\omega \in [0, \frac{\pi}{T})$ is the alias of the sidebands $k\frac{2\pi}{T} \pm \omega$, with $k \in \mathbb{N}^+$, and all frequencies above the Nyquist frequency $\frac{\pi}{T}$ will distort the baseband spectrum after sampling. Although sampling is a linear operation, it is not time invariant, which explains why new frequencies are created by the sampling [2]. Note that the sampling operation has a gain of $1/T$.

The inverse of the sampling operation is the so-called Shannon reconstruction, which perfectly reconstructs the baseband $\omega \in [0, \frac{\pi}{T})$ of the discrete-time signal into a continuous-time signal. Unfortunately, this operation is not causal—hence inappropriate for real-time applications—and complicated to realise [2,3]. The zero-order hold is a very simple and causal reconstruction, and is therefore most commonly used in control systems [2–5]. Its pulse transfer function is

$$G_{\mathrm{ZOH}}(s) = \frac{1 - e^{-sT}}{s}. \tag{2}$$

The harmonic transfer function at $s = j\omega$

$$G_{\mathrm{ZOH}}(j\omega) = T\frac{\sin\omega\frac{T}{2}}{\omega\frac{T}{2}}e^{-j\omega\frac{T}{2}} \tag{3}$$

shows that the zero-order hold reconstruction causes some distortion of the baseband and only has a first-order attenuation of the sidebands, and that it contains a pure delay of half the sampling period. Using Tustin's approximation

$$e^{sT} \approx \frac{1 + s\frac{T}{2}}{1 - s\frac{T}{2}}, \tag{4}$$

the zero-order hold is equivalent to a first-order system

$$G_{\mathrm{ZOH}}(s) \approx T\frac{1}{s\frac{T}{2} + 1} \tag{5}$$

with a time constant of half the sampling period [5]. Note that reconstruction has a dc gain of T.

3 Sampling Period

Selection of the sampling period is an important issue in digital control. Different authors give different selection criteria for the sampling period T or frequency $1/T$, which are summarised in Table 1. The choice is related to the bandwidth[2] of the closed-loop system f_b. The criterion

$$\frac{1/T}{f_b} \in [10, 25] \tag{6}$$

is a reasonable consensus among the different authors. Especially the lower bound is critical, the upper bound is not. Although the error due to load disturbances increases with increasing sampling period due to the inherent delay in observing and reacting to a disturbance, it is important to chose the sampling frequency rather low. Higher sampling frequencies increase the precision requirements on the controller implementation (coefficients and/or state variables) and might increase the order of the process model—especially in presence of delay—, which in turn increases sensitivity to modelling errors.

[2]The bandwidth roughly equals the natural frequency, which is the frequency of the dominant pole(s).

Table 1: Selection criteria for sampling period ($\omega_b = 2\pi f_b$).

author	criterion	$\omega_b T$	$1/f_b T$
Åström & Wittenmark [2]	$0.2 \leq \omega_b T \leq 0.6$	$0.2 \ldots 0.6$	$10 \ldots 30$
Longchamp [3]	$10 f_b \leq 1/T \leq 20 f_b$	$0.3 \ldots 0.6$	$10 \ldots 20$
Landau [4]	$6 f_b \leq 1/T \leq 25 f_b$	$0.25 \ldots 1.0$	$6 \ldots 25$
Bühler [5]	real: $T \leq 1/2\omega_b$	$0 \ldots 0.5$	$12 \ldots \infty$
	complex: $T \leq \pi/4\omega_b$	$0 \ldots 0.8$	$8 \ldots \infty$

4 Antialiasing Filter

If the signal to be sampled contains frequencies above the Nyquist frequency that will distort the sampled signal due to aliasing and if these distortions will degrade the performance of the control, those frequencies must be removed by appropriately filtering the signal prior to sampling. Such a filter is called an antialiasing filter.

Antialiasing filters should be carefully designed. Any (causal) filtering introduces delay, and, generally, stronger filtering produces more delay. Because any delay in the loop reduces the possible control performance, antialiasing filters should be reduced to a strict minimum. Filtering can be omitted where the signal to be sampled has sufficiently small noise or where aliased sideband frequencies will not degrade performance (e.g. while remaining outside the closed-loop passband). A 'default' antialiasing filter with important attenuation above the Nyquist frequency has major delay, and its use is strongly discouraged for high-performance control applications.

To design a high-performance controller, antialiasing-filter dynamics must be included in the process model. As long as the filter's bandwidth is greater than the closed-loop bandwidth, its dynamics can be approximated with a pure delay equal to its group delay.

5 Process Model

The relation between the discrete-time transfer function $H(z)$ and the continuous-time transfer function $G(s)$ of a process depends on the shape of the analogue control signal between sampling instants. Holding the signal constant (zero-order hold) is most common in digital control because of its simplicity. For this case, the relation between the discrete- and continuous-time transfer functions is

$$H(z) = \frac{z-1}{z} \mathcal{Z} \left\{ \mathcal{L}^{-1} \left[\frac{G(s)}{s} \right] \right\}, \tag{7}$$

where $\mathcal{L}$ and $\mathcal{Z}$ denote the Laplace and the Z-transform respectively [2, 3]. In practice, the measured process output is not influenced by the controlled process input at the same sampling instant, even if the continuous-time system has a direct term [2, 3]. This results in a one sample delay for any direct term and a transfer function whose numerator polynomial has a lower degree than its denominator polynomial.

Ramping the signal linearly (first-order hold) is an approximation when the system is driven by a slowly varying continuous-time signal. For this case, the relation between the discrete- and continuous-time transfer functions is

$$H'(z) = \frac{(z-1)^2}{Tz} \mathcal{Z} \left\{ \mathcal{L}^{-1} \left[\frac{G(s)}{s^2} \right] \right\}. \tag{8}$$

For a process that is the cascade of two systems

$$G(s) = G_2(s) G_1(s), \tag{9}$$

the exact discrete-time transfer function corresponds to (7) applied to the whole system. However, if the first subsystem G_1 has a bandwidth $\omega_{b,1}$ that is either much bigger or much smaller than the sampling frequency, the discrete-time transfer function can be approximated as

$$H(z) \approx \begin{cases} H_2'(z) H_1(z) & \omega_{b,1} T \ll 1 \\ H_2(z) H_1(z) & \omega_{b,1} T \gg 1 \end{cases}. \tag{10}$$

The first subsystem is driven by a zero-order hold from the controller, whereas the second subsystem is driven either by a first-order hold from a slow first subsystem, or by a zero-order hold from a fast first subsystem.

To evaluate (7) or (8) for proper rational transfer functions $G(s)$, we can express the function $F(s)$—which equals $G(s)/s$ or $G(s)/s^2$—as a sum of partial fractions [1, 3, 7]. The terms associated to any pole $s = -a$ of $F(s)$ with multiplicity ℓ are

$$\frac{c_1}{s+a} + \frac{c_2}{(s+a)^2} + \cdots + \frac{c_\ell}{(s+a)^\ell}, \quad c_k = \frac{1}{(\ell-k)!} \frac{\mathrm{d}^{\ell-k} F(s)(s+a)^\ell}{\mathrm{d}s^{\ell-k}}\bigg|_{s=-a}, \tag{11}$$

with well-known inverse Laplace transforms [1, 7]. The Z-transforms corresponding to these terms are available in the literature, such as [2, 3, 7, 8], and can be expressed as

$$\frac{c_1 z}{z - e^{-aT}} + \frac{c_2 T e^{-aT} z}{(z - e^{-aT})^2} + \cdots + \frac{c_\ell (-1)^{\ell-1}}{(\ell-1)!} \cdot \frac{\partial^{\ell-1}}{\partial a^{\ell-1}} \left(\frac{z}{z - e^{-aT}} \right) \tag{12}$$

according to [3].

6 Process Model with Delay

The continuous-time transfer function of a process that contains a pure delay is

$$G(s) = e^{-sdT} G_0(s), \tag{13}$$

where dT is the delay expressed as a multiple d of the sampling period T. For integer delays, the corresponding discrete-time transfer function is

$$H(z) = z^{-d} H_0(z), \quad d \in \mathbb{N}. \tag{14}$$

For non-integer delays, the corresponding discrete-time transfer function is more laborious to calculate [2]. However, if the process G_0 has a bandwidth $\omega_{b,0}$ that is much smaller than the sampling frequency, the discrete-time transfer function can be approximated as

$$H(z) \approx H_d(d, z) H_0(z), \quad \omega_{b,0} T \ll 1, \tag{15}$$

where the delay function[3]

$$H_d(d, z) = z^{-\lfloor d \rfloor} \left(1 - (d - \lfloor d \rfloor) + (d - \lfloor d \rfloor) z^{-1} \right), \quad d \in \mathbb{R}. \tag{16}$$

corresponds to a linear interpolation between two samples—the current and the previous one $H_d(d, z) = (1-d) + dz^{-1}$ for $d \in [0, 1]$, more prior ones for bigger delays. If the process G_0 has a bandwidth $\omega_{b,0}$ that is much bigger than the sampling frequency, the discrete-time transfer function can be approximated with the delay function only

$$H(z) \approx \begin{cases} H_d(z, \tau_G/T) & \text{first-order hold} \\ H_d(z, \lceil \tau_G/T \rceil) & \text{zero-order hold} \end{cases}, \quad \omega_{b,0} T \gg 1, \tag{17}$$

parametrised at the process' dc group delay $\tau_G = -\mathrm{d}\angle G(j\omega)/\mathrm{d}\omega|_{\omega=0}$ with respect to the sampling period for a first-order hold discretization, respectively at its ceiling for a zero-order hold discretization.

7 Control Stability and Robustness

The Nyquist criterion determines the stability of the closed-loop system from the open-loop transfer function $G_l(s)$ respectively $H_l(z)$. The criterion states that the closed-loop system is stable if and only if the Nyquist curve (the frequency-response curve in the complex plane) of the open-loop system $G_l(j\omega)$ with $\omega \in (-\infty, +\infty)$ respectively $H_l(e^{j\omega T})$ with $\omega T \in [-\pi, +\pi]$ encircles the critical point -1 in the positive direction with increasing ω as many times as it has unstable poles (those in the right-hand plane $\Re s > 0$ for continuous-time systems respectively outside the unit disc $|z| > 1$ for discrete-time systems); it should be assumed that the phasor travels ℓ times a semicircle of infinite radius in the negative direction at the discontinuity $\omega = 0$ if the open-loop transfer function has ℓ integrator poles (at $s = 0$ for continuous-time systems respectively $z = 1$ for discrete-time systems). A common case in practice, the open-loop system has no unstable poles and the Nyquist curve must not encircle the critical point to obtain a stable closed-loop system (the critical point is to the left of the Nyquist curve) [1–3].

[3] The notations $\lfloor x \rfloor$ and $\lceil x \rceil$ denote the floor and ceiling functions, which map the real number x to the largest integer not greater than x respectively the smallest integer not less than x.

For a control system to be robust against modelling errors and parameter variations and uncertainties, the Nyquist curve must remain at sufficient distance from the critical point. The modulus margin

$$m_m = \begin{cases} \min |1 + G_l(j\omega)| & \text{continuous time} \\ \min \left|1 + H_l(e^{j\omega T})\right| & \text{discrete time} \end{cases} \tag{18}$$

is the minimum value of this distance [9,10]. Note that the classical gain and phase margins represent this distance only at the two points where the Nyquist curve's argument equals π or magnitude equals 1; the Nyquist curve could come very close to the critical point elsewhere.

A common robustness criterion is that the modulus margin respects

$$m_m \geq 0.5 \quad \Leftrightarrow \quad 20 \log_{10} \frac{1}{m_m} \leq 6\,\text{dB}. \tag{19}$$

These criteria can be verified by drawing a circle with radius 0.5 around the critical point on the Nyquist diagram of G_l respectively H_l, or by drawing a horizontal line at $6\,\text{dB}$ on the Bode magnitude diagram of $1/(1 + G_l)$ respectively $1/(1 + H_l)$. Note that a modulus margin $m_m \geq 0.5$ ensures gain and phase margins of at least $g_m \geq 20 \log_{10} \frac{1}{1-m_m} \geq 6\,\text{dB}$ and $\phi_m \geq 2 \arcsin \frac{m_m}{2} \geq 29°$ respectively.

...

8 Compensation of Process Nonlinearity

...

9 RST-Controller

An RST-controller uses three polynomials

$$R(z) = r_0 z^\rho + r_1 z^{\rho-1} + \cdots + r_\rho \tag{20}$$
$$S(z) = s_0 z^\sigma + s_1 z^{\sigma-1} + \cdots + s_\sigma \tag{21}$$
$$T(z) = t_0 z^\tau + t_1 z^{\tau-1} + \cdots + t_\tau \tag{22}$$

of degrees ρ, σ and τ respectively, with $R(z)$ monic ($r_0 = 1$). The control law[4] is defined as

$$R(z)U(z) = T(z)W(z) - S(z)Y(z), \tag{23}$$

with $U(z)$ the control signal, $Y(z)$ the measured process signal, and $W(z)$ the command signal in the z-domain [2,3]. Figure 2 shows the RST-controller. To obtain a causal controller, the degrees of $S(z)$ and $T(z)$ may not exceed that of $R(z)$, thus $\sigma \leq \rho$ and $\tau \leq \rho$.

For the implementation of an RST-controller, its control law must be expressed using negative powers of z. Using $\rho = \sigma = \tau = n$ and dividing (20)–(23) by z^n, we obtain

$$R'(z^{-1}) = r_0 + r_1 z^{-1} + \cdots + r_n z^{-n} \tag{24}$$
$$S'(z^{-1}) = s_0 + s_1 z^{-1} + \cdots + s_n z^{-n} \tag{25}$$
$$T'(z^{-1}) = t_0 + t_1 z^{-1} + \cdots + t_n z^{-n} \tag{26}$$

[4] Our notation follows Åström & Wittenmark [2] and Longchamp [3]; it does *not* follow Landau [4], who unfortunately swaps the R and S polynomials. The chosen notation corresponds to the widespread convention that the first character of a series is used for the denominator polynomial, as in B/A.

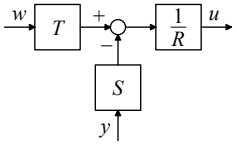

Figure 2: RST-controller.

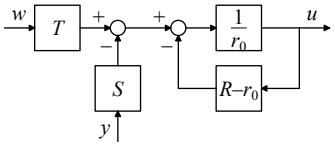

Figure 3: RST-controller implementation.

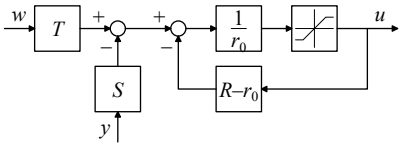

Figure 4: RST-controller implementation with control saturation.

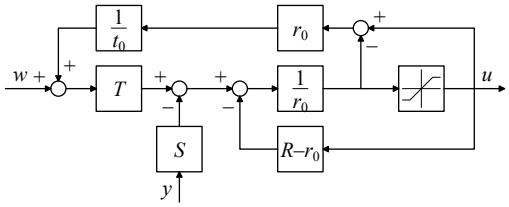

Figure 5: RST-controller implementation with control saturation and command correction.

and

$$R'(z^{-1})U(z) = T'(z^{-1})W(z) - S'(z^{-1})Y(z), \tag{27}$$

which can be rewritten as

$$r_0 U(z) = T'(z^{-1})W(z) - S'(z^{-1})Y(z) - [R'(z^{-1}) - r_0]U(z). \tag{28}$$

Because the polynomial $[R'(z^{-1}) - r_0]$ contains a factor z^{-1}, this expression can be evaluated in the time domain by replacing factors z^{-1} with backward time shifts (delays). An RST-controller of order n can thus be implemented as

$$u(k) = \frac{1}{r_0}\left[t_0 w(k) - s_0 y(k) + \sum_{i=1}^{n} t_i w(k-i) - s_i y(k-i) - r_i u(k-i)\right], \tag{29}$$

with $u(k)$ the control signal, $y(k)$ the measured process signal, and $w(k)$ the command signal at sample k [3]. The coefficients are effectively normalised to $r_0 = 1$. Figure 3 shows the RST-controller implementation. In case of a computing delay of one sample, the coefficients s_0 and t_0 must equal zero. Alternatively, such a delay can be included in the process model instead of in the controller. The latter approach allows to use the normal controller synthesis and associates the samples $u(k)$, $y(k)$ and $w(k)$ with the k^{th} call of the controller execution routine, whereas the former approach requires a modified synthesis and associates $u(k+1)$, $y(k)$ and $w(k)$ with the k^{th} call.

In practice, the control signal must be amplified to drive the system under control. The amplifier will have limitations and for fast large command-signal variations (e.g. steps), the control signal might saturate. To avoid integrator windup, the effectively applied (i.e. saturated) control signal should be used in the RST-controller history instead of the calculated (i.e. unsaturated) one, as shown in Figure 4 [2]. This solution corresponds to tracking the control signal to its saturation, which occurs with certain dynamics intrinsic to the controller. To avoid these dynamics, also an 'effectively applied' command signal should be used in the RST-controller history (instead of the original one), which corresponds to the command that drives the controller exactly to the boundary between the linear and the saturated regions. To remain in the linear region, (29) must also be respected for the saturated control and command signals $u'(k)$ and $w'(k)$. Subtracting the saturated and unsaturated versions of (29) results in the effectively applied command signal

$$w'(k) = w(k) + \frac{r_0}{t_0}[u'(k) - u(k)]. \tag{30}$$

Figure 5 shows the RST-controller implementation with control saturation and command correction.

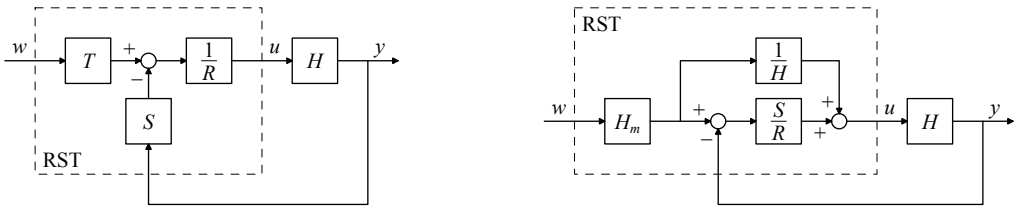

(a) Implementation (b) Synthesis

Figure 6: RST-controller with process.

10 RST-Controller Synthesis

The synthesis[5] of an RST-controller aims to obtain a chosen closed-loop transfer function $H_m(z) = B_m(z)/A_m(z)$ for a given process open-loop transfer function $H(z) = B(z)/A(z)$ (with $\deg A > \deg B$). Although the controller implementation is as shown in Figure 6a, the synthesis results in an equivalent controller as shown in Figure 6b [2, 3].

The choice of H_m must respect the following two constraints. To obtain a causal controller, the pole excess of the model H_m must be at least as large as that of the process H:

$$\deg A_m - \deg B_m \geq \deg A - \deg B. \tag{31}$$

Zeros of the open-loop transfer function can only disappear from the closed-loop transfer function by cancelling them with controller poles. To avoid insufficiently damped or even unstable internal modes, only zeros of the process transfer function $H(z)$ corresponding to modes with sufficient absolute and relative damping may be cancelled by controller poles, the others must be included in the closed-loop transfer function $H_m(z)$. If B^+ contains the zeros to be cancelled and B^- contains the zeros to be kept (with B^+ monic), the numerators of the open-loop and closed-loop transfer functions are

$$B = B^+ B^-, \tag{32}$$

$$B_m = B^- B'_m, \tag{33}$$

where B'_m contains the desired (additional) zeros of $H_m(z)$. Note that B^+ must be a factor of R.

Load disturbances can be eliminated by introducing suitable factors $R^*(z)$ in the polynomial $R(z)$. The classical principle of integral control can be achieved by using

$$R^*(z) = (z-1)^\ell \tag{34}$$

with a suitable ℓ [2, 3]. This eliminates a constant (or other polynomial) load disturbance by setting $R(1) = 0$. Elimination of a load disturbance with frequency ω can be obtained by a factor

$$R^*(z) = z^2 - 2z\cos\omega T + 1 \tag{35}$$

setting $R(e^{\pm j\omega T}) = 0$ [2]. Similarly, notch-filter effects can be obtained by introducing suitable factors $S^*(z)$ in the polynomial $S(z)$. A factor

$$S^*(z) = z^2 - 2z\cos\omega T + 1 \tag{36}$$

setting $S(e^{\pm j\omega T}) = 0$ filters signals in the output with frequency ω [2, 3].

$$R = B^+ R^* R' \tag{37}$$

$$S = S^* S' \tag{38}$$

$$T = B'_m A_o \tag{39}$$

The existence of a solution requires that the order of the observer polynomial respects

$$\deg A_o \geq 2\deg A - \deg A_m - \deg B^+ + \deg R^* + \deg S^* - 1. \tag{40}$$

[5] Our synthesis follows Åström & Wittenmark [2] and Longchamp [3] and uses polynomials in z, because all closed-loop poles are explicitly placed. The synthesis by Landau [4] using polynomials in z^{-1} is not recommended, because additional poles might implicitly be placed in the origin.

$$B = B^+ B^- \tag{41}$$
$$B_m = B^- B'_m \tag{42}$$
$$\deg A_m - \deg B_m \geq \deg A - \deg B \tag{43}$$
$$\deg A_o \geq 2\deg A - \deg A_m - \deg B^+ + \deg R^* + \deg S^* - 1 \tag{44}$$
$$AR^*R' + B^- S^* S' = A_m A_o \tag{45}$$
$$\deg R' = \deg A_m + \deg A_o - \deg A - \deg R^* \geq \deg A - \deg B^+ - 1 \tag{46}$$
$$\deg S' = \deg A + \deg R^* - 1 \tag{47}$$
$$R = B^+ R^* R' \tag{48}$$
$$S = S^* S' \tag{49}$$
$$T = B'_m A_o \tag{50}$$

11 RST-Controller Synthesis for PID-Control

Classical PID-control can be implemented using an RST-controller [2–4]. The theoretic PID-control law is

$$U(s) = K\left[1 + \frac{1}{s\tau_i} + s\tau_d\right][W(s) - Y(s)], \tag{51}$$

with $U(s)$ the control signal, $Y(s)$ the measured process signal, and $W(s)$ the command signal in the s-domain. The parameters are the proportional gain K, the integration time τ_i, and the differentiation time τ_d.

In practice, it is useful to let only a fraction $b \in [0, 1]$ of the command act on the proportional part and none of it on the derivative part, which allows to place the closed-loop zeros separately [2]. To avoid amplification of measurement noise, the high-frequency gain of the derivative part should be limited to $N \in [3, 20]$, which can be achieved by including a filter with time constant τ_d/N [2–4]. The resulting PID-control law becomes

$$U(s) = K\left[bW(s) - Y(s) + \frac{1}{s\tau_i}[W(s) - Y(s)] - \frac{s\tau_d}{s\frac{\tau_d}{N} + 1}Y(s)\right]. \tag{52}$$

Discretisation of (52) with Euler's second (backward) method $s = \frac{z-1}{zT}$ and writing it in RST-form (23) results in

$$R(z) = z^2 - (1 + a_d)z + a_d = (z - 1)(z - a_d), \tag{53}$$
$$S(z) = K\left[(1 + b_i + b_d)z^2 - (1 + a_d + b_i a_d + 2b_d)z + (a_d + b_d)\right], \tag{54}$$
$$T(z) = K\left[(b + b_i)z^2 - (b + ba_d + b_i a_d)z + ba_d\right] = K((b + b_i)z - b)(z - a_d), \tag{55}$$

with

$$a_d = \frac{\tau_d}{\tau_d + NT}, \tag{56}$$
$$b_d = Na_d, \tag{57}$$
$$b_i = \frac{T}{\tau_i}. \tag{58}$$

Euler's second method ensures that the filter pole $0 \leq a_d < 1$ is always stable.

A special case is obtained if the reference acts only on the integral part. Setting $b = 0$ results in

$$T(z) = K\left[b_i z^2 - b_i a_d z\right] = Kb_i(z - a_d)z. \tag{59}$$

For the command signal, one zero is placed at the filter pole and the other at the origin.

A special discretisation method is often applied, with Euler's second (backward) method $s = \frac{z-1}{zT}$ for the derivative part and Euler's first (forward) method $s = \frac{z-1}{T}$ for the integral part [2, 3]. In this case, all terms with the factor b_i move to one degree lower in z.

Another special method places all zeros of $T(z)$ in the origin [4]. Preserving the dc gain, this results in

$$T'(z) = T(1)z^2 = Kb_i(1 - a_d)z^2, \tag{60}$$

Table 2: RST-coefficients for PID-control.

coefficient	PI(D) control	PD control
a_d	$\tau_d/(\tau_d + NT)$	
b_d	Na_d	
b_i	T/τ_i	
r_0	1	1
r_1	$-(1 + a_d)$	$-a_d$
r_2	a_d	0
s_0	$K(1 + b_i + b_d)$	$K(1 + b_d)$
s_1	$-K(1 + a_d + b_i a_d + 2b_d)$	$-K(a_d + b_d)$
s_2	$K(a_d + b_d)$	0
t_0	$K(b + b_i)$	$K(b)$
t_1	$-K(b + ba_d + b_i a_d)$	$-K(ba_d)$
t_2	$K(ba_d)$	0
t'_0	$Kb_i(1 - a_d)$	$Kb(1 - a_d)$
t'_1	0	0
t'_2	0	0

Table 3: Selection criteria for sampling period with PID-control.

author	control	criterion
Åström & Wittenmark [2]	PI	$0.1 \leq T/\tau_i \leq 0.3$
	P(I)D	$0.2 \leq T/(\tau_d/N) \leq 0.6$

which is equivalent to $t'_0 = \sum_n t_n$ and $t'_n = 0 \; \forall n > 0$. This corresponds to a command which acts only on the integral part and is additionally filtered by the filter pole a_d.

In many applications, PI-control is used without a derivative term. Setting $\tau_d = 0$ leads to $a_d = 0$ and $b_d = 0$ and results in

$$R(z) = z^2 - z \qquad = (z-1)z \tag{61}$$

$$S(z) = K\left[(1 + b_i)z^2 - z\right] = K((1 + b_i)z - 1)z \tag{62}$$

$$T(z) = K\left[(b + b_i)z^2 - bz\right] = K((b + b_i)z - b)z. \tag{63}$$

The common factor z poses no problem, since all last coefficients become zero ($r_2 = 0$, $s_2 = 0$, $t_2 = 0$). The general equations for PID-control can thus be used.

In some applications, PD-control is used without an integral term. Setting $\tau_i = \infty$ leads to $b_i = 0$ and results in

$$R(z) = z^2 - (1 + a_d)z + a_d \qquad = (z-1)(z-a_d) \tag{64}$$

$$S(z) = K\left[(1 + b_d)z^2 - (1 + a_d + 2b_d)z + (a_d + b_d)\right] = K(z-1)((1 + b_d)z - (a_d + b_d)) \tag{65}$$

$$T(z) = K\left[bz^2 - (b + ba_d)z + ba_d\right] \qquad = Kb(z-1)(z-a_d). \tag{66}$$

The common factor $z - 1$ is problematic, because it is an unstable pole-zero cancellation. A stable controller is obtained by dividing it out ($r'_0 = r_0$, $r'_1 = -r_2$, $r'_2 = 0$, etc.).

The RST-coefficients for the different cases of PID-control are summarised in Table 2.

In case of PID-control, some rules of thumb for selection of the sampling period are given in the literature. They are summarised in Table 3.

12 General Magnet Load Model

Magnets are modelled as an inductance L_m with a series resistance R_m. The load can include a parallel resistance R_p and/or a series resistance R_s. Figure 7 shows the general magnet load circuit model. The continuous-time transfer function from the voltage to the current of this load is

$$G(s) = \frac{1}{R_s + \dfrac{1}{\dfrac{1}{R_p} + \dfrac{1}{R_m + sL_m}}}, \tag{67}$$

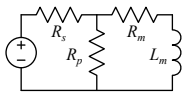

Figure 7: General magnet load circuit model.

which can be written as

$$G(s) = g_0 + g_1 \frac{1}{s\tau + 1}, \quad \begin{cases} \tau = \dfrac{L_m}{R_m + \frac{R_p R_s}{R_p + R_s}} & = \dfrac{L_m}{R_m + \frac{R_s}{1 + R_s R_p^{-1}}}, \\ g_0 = \dfrac{1}{R_s + R_p} & = \dfrac{R_p^{-1}}{1 + R_s R_p^{-1}}, \\ g_1 = \dfrac{1}{R_s + \frac{R_p R_m}{R_p + R_m}} - \dfrac{1}{R_s + R_p} & = \dfrac{1}{R_s + \frac{R_m}{1 + R_m R_p^{-1}}} - \dfrac{R_p^{-1}}{1 + R_s R_p^{-1}}. \end{cases} \tag{68}$$

For an analogue control signal that is constant between sampling instants (zero-order-hold), the discrete-time transfer function of this load is

$$H(z) = g_0 \frac{1}{z} + g_1 \frac{1 - e^{-T/\tau}}{z - e^{-T/\tau}}, \tag{69}$$

which can be written as

$$H(z) = \frac{b_0 z + b_1}{z(z + a_1)}, \quad \begin{cases} a_1 = -e^{-T/\tau}, \\ b_0 = g_0 + g_1(1 - e^{-T/\tau}), \\ b_1 = -g_0 e^{-T/\tau}. \end{cases} \tag{70}$$

The zero of this transfer function is

$$\text{zero}(H) = -\frac{b_1}{b_0} = 1 - \frac{(g_0 + g_1)(1 - e^{-T/\tau})}{g_0 + g_1(1 - e^{-T/\tau})} \in (0, 1), \tag{71}$$

which is always located inside the unit circle.

For an analogue control signal that is linear between sampling instants (first-order-hold), the discrete-time transfer function of this load is

$$H(z) = g_0 + g_1 \frac{(1 - \frac{1 - e^{-T/\tau}}{T/\tau})z - (e^{-T/\tau} - \frac{1 - e^{-T/\tau}}{T/\tau})}{z - e^{-T/\tau}}, \tag{72}$$

which can be written as

$$H(z) = \frac{b_0 z + b_1}{z + a_1}, \quad \begin{cases} a_1 = -e^{-T/\tau}, \\ b_0 = g_0 + g_1(1 - \dfrac{1 - e^{-T/\tau}}{T/\tau}), \\ b_1 = -g_0 e^{-T/\tau} - g_1(e^{-T/\tau} - \dfrac{1 - e^{-T/\tau}}{T/\tau}). \end{cases} \tag{73}$$

The zero of this transfer function is

$$\text{zero}(H) = -\frac{b_1}{b_0} = 1 - \frac{(g_0 + g_1)(1 - e^{-T/\tau})}{g_0 + g_1(1 - \frac{1 - e^{-T/\tau}}{T/\tau})} \in (-1, +1), \tag{74}$$

which is always located inside the unit circle.

For sampling periods that are small compared to the process time constant, we can approximate the exponential term as

$$T \ll \tau \quad \Rightarrow \quad e^{-T/\tau} \approx 1 - T/\tau, \tag{75}$$

with an error of about $(T/\tau)^2/2$. This approximation is allowed if T/τ is smaller than the uncertainty in the model parameters, because the error in $1 - e^{-T/\tau}$ will be smaller than the uncertainty.

In certain applications, some resistances in the general magnet load model may vanish (except that R_m and R_s may not vanish together).

No magnet resistance

$$R_m = 0 \quad \Rightarrow \quad \tau = \frac{L_m}{R_p} + \frac{L_m}{R_s}, \quad g_0 = \frac{1}{R_s + R_p}, \quad g_1 = \frac{1}{R_s} - \frac{1}{R_s + R_p}, \tag{76}$$

$$R_m = 0 \quad \Rightarrow \quad a_1 = -e^{-T/\tau}, \quad b_0 = \frac{1 + \frac{R_p}{R_s}(1 - e^{-T/\tau})}{R_s + R_p}, \quad b_1 = -\frac{e^{-T/\tau}}{R_s + R_p}. \tag{77}$$

No series resistance

$$R_s = 0 \quad \Rightarrow \quad \tau = \frac{L_m}{R_m}, \quad g_0 = \frac{1}{R_p}, \quad g_1 = \frac{1}{R_m}. \tag{78}$$

$$R_s = 0 \quad \Rightarrow \quad a_1 = -e^{-T/\tau}, \quad b_0 = \frac{1 + \frac{R_p}{R_m}(1 - e^{-T/\tau})}{R_p}, \quad b_1 = -\frac{e^{-T/\tau}}{R_p}. \tag{79}$$

No parallel resistance

$$R_p = \infty \quad \Rightarrow \quad \tau = \frac{L_m}{R_m + R_s}, \quad g_0 = 0, \quad g_1 = \frac{1}{R_m + R_s}, \tag{80}$$

$$R_p = \infty \quad \Rightarrow \quad a_1 = -e^{-T/\tau}, \quad b_0 = \frac{1}{R_m + R_s}(1 - e^{-T/\tau}), \quad b_1 = 0. \tag{81}$$

Only the sum $R_m + R_s$ is relevant for the transfer function. The direct term vanishes and the continuous-time transfer function becomes a pure first-order one, and the discrete-time transfer function simplifies to

$$R_p = \infty \quad \Rightarrow \quad H(z) = \frac{b_0}{z + a_1}. \tag{82}$$

The zero and the pole in the origin have disappeared.

No magnet resistance and no series resistance

$$G(s) = \frac{1}{R_p} + \frac{1}{sL_m}, \tag{83}$$

which can be written as

$$G(s) = g_0 + g_1 \frac{1}{s}, \quad \begin{cases} g_0 = \dfrac{1}{R_p}, \\ g_1 = \dfrac{1}{L_m}. \end{cases} \tag{84}$$

$$H(z) = g_0 \frac{1}{z} + g_1 \frac{T}{z - 1}, \tag{85}$$

which can be written as

$$H(z) = \frac{b_0 z + b_1}{z(z-1)}, \quad \begin{cases} b_0 = g_0 + g_1 T = \dfrac{1}{R_p} + \dfrac{T}{L_m}, \\ b_1 = -g_0 \qquad\quad = -\dfrac{1}{R_p}. \end{cases} \tag{86}$$

The zero of this transfer function is

$$\text{zero}(H) = -\frac{b_1}{b_0} = \frac{1}{1 + T/\frac{L_m}{R_p}} \in (0, 1), \tag{87}$$

which is always located inside the unit circle.

13 Compensation of Magnet Saturation

...

14 Simulation Model

Magnet Saturation:

$$L_m(i_m) = l_m(i_m)L_m(0) \quad \Rightarrow \quad \tau(i_m) = l_m(i_m)\tau(0) \tag{88}$$

Magnet current:

$$i_m = i - \frac{u - R_s i}{R_p} = (1 + R_s R_p^{-1})(i - g_0 u) \tag{89}$$

Fast voltage source ($T \gg 1/\omega_b$, zero-order hold of load):

$$i(k) = b_0 u(k-1) + b_1 u(k-2) - a_1 i(k-1) \tag{90}$$

or (with smaller numerical error):

$$i'(k) = i'(k-1) + [1 - e^{-T/\tau}][g_1 u(k-1) - i'(k-1)] \tag{91}$$

$$i(k) = i'(k) + g_0 u(k-1) \tag{92}$$

Slow load ($T \ll \tau$, $1 - e^{-T/\tau} \approx \frac{T}{\tau}$) and magnet saturation:

$$i'(k) \approx i'(k-1) + \tfrac{1}{l_m(i_m(k-1))} \tfrac{T}{\tau(0)} [g_1 u(k-1) - i'(k-1)] \tag{93}$$

$$i(k) = i'(k) + g_0 u(k-1) \tag{94}$$

$$i_m(k) = (1 + R_s R_p^{-1}) i'(k) \tag{95}$$

Slow voltage source ($T \ll 1/\omega_b$, first-order hold of load):

$$i(k) = b_0 u(k) + b_1 u(k-1) - a_1 i(k-1) \tag{96}$$

or (with smaller numerical error):

$$i'(k) = i'(k-1) + [1 - e^{-T/\tau}][g_1 u(k-1) - i'(k-1)] + [1 - \tfrac{1-e^{-T/\tau}}{T/\tau}][g_1 u(k) - g_1 u(k-1)] \tag{97}$$

$$i(k) = i'(k) + g_0 u(k) \tag{98}$$

Slow load ($T \ll \tau$, $1 - e^{-T/\tau} \approx \frac{T}{\tau}$, $1 - \frac{1-e^{-T/\tau}}{T/\tau} \approx \frac{T}{2\tau}$) and magnet saturation:

$$i'(k) \approx i'(k-1) + \tfrac{1}{l_m(i_m(k-1))} \tfrac{T}{\tau(0)} [g_1 \tfrac{u(k)+u(k-1)}{2} - i'(k-1)] \tag{99}$$

$$i(k) = i'(k) + g_0 u(k) \tag{100}$$

$$i_m(k) = (1 + R_s R_p^{-1}) i'(k) \tag{101}$$

$$R_s = 0 \qquad \Rightarrow \qquad i_m = i' \tag{102}$$

$$R_p = \infty \qquad \Rightarrow \qquad i = i_m = i' \tag{103}$$

15 Example: LHC Power Converters with Control Delay

LHC Magnet Load Model

The loads of the LHC power converters are modelled as an inductance L with a series resistance R_s and, for some cases, a parallel resistance R_p, as shown in Figure 8 [11,12]. The continuous-time transfer function from the voltage to the current of this load is

$$G(s) = \frac{1}{R_s} \frac{s\frac{L}{R_p} + 1}{s\frac{L(R_s+R_p)}{R_s R_p} + 1}, \tag{104}$$

which can be written as

$$G(s) = g_0 + g_1 \frac{1}{s\tau + 1}, \quad \begin{cases} \tau = \dfrac{L}{R_s} + \dfrac{L}{R_p}, \\ g_0 = \dfrac{1}{R_s + R_p}, \\ g_1 = \dfrac{1}{R_s} - \dfrac{1}{R_s + R_p}. \end{cases} \tag{105}$$

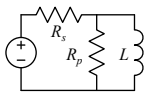

Figure 8: LHC circuit model.

For the cases without a parallel resistance, we get

$$R_p \to \infty \quad \Rightarrow \quad \tau = \frac{L}{R_s}, \quad g_0 = 0, \quad g_1 = \frac{1}{R_s}. \tag{106}$$

The direct term vanishes and the transfer function becomes a pure first-order one.

For an analogue control signal that is constant between sampling instants (zero-order-hold), the discrete-time transfer function of the load is

$$H(z) = g_0 \frac{1}{z} + g_1 \frac{1 - e^{-T/\tau}}{z - e^{-T/\tau}}, \tag{107}$$

which can be written as

$$H(z) = \frac{b_0 z + b_1}{z(z + a_1)}, \quad \begin{cases} a_1 = -e^{-T/\tau}, \\ b_0 = g_0 + g_1(1 - e^{-T/\tau}) = \dfrac{1 + \frac{R_p}{R_s}(1 - e^{-T/\tau})}{R_s + R_p}, \\ b_1 = -g_0 e^{-T/\tau} \qquad\quad = \dfrac{-e^{-T/\tau}}{R_s + R_p}. \end{cases} \tag{108}$$

The zero of this transfer function is

$$\mathrm{zero}(H) = -\frac{b_1}{b_0} = 1 - \frac{(g_0 + g_1)(1 - e^{-T/\tau})}{g_0 + g_1(1 - e^{-T/\tau})} = 1 - \frac{(R_s + R_p)(1 - e^{-T/\tau})}{R_s + R_p(1 - e^{-T/\tau})} \in (0, 1), \tag{109}$$

which is always located inside the unit circle. For the cases without a parallel resistance, we get

$$R_p \to \infty \quad \Rightarrow \quad a_1 = -e^{-T/\tau}, \quad b_0 = g_1(1 - e^{-T/\tau}) = \frac{1}{R_s}(1 - e^{-T/\tau}), \quad b_1 = 0, \tag{110}$$

and the transfer function simplifies to

$$R_p \to \infty \quad \Rightarrow \quad H(z) = \frac{b_0}{z + a_1}. \tag{111}$$

The zero and the pole in the origin have disappeared.

If there is a delay in the control loop—either in the actuation or in the acquisition, or both together—the transfer function of the system has to be adapted accordingly. For a total delay dT that is a fraction $d \in [0, 1)$ of the sampling period T, the discrete-time transfer function of the load can be modelled as

$$H(z) = g_0 \frac{1}{z} + g_1 \frac{1 - e^{-T/\tau}}{z - e^{-T/\tau}} \frac{(1 - d)z + d}{z}, \tag{112}$$

$$H(z) = g_0 \frac{1}{z} + g_1 \frac{(1 - e^{-(1-d)T/\tau})z + (e^{-(1-d)T/\tau} - e^{-T/\tau})}{z(z - e^{-T/\tau})}, \tag{113}$$

which can be written as

$$H(z) = \frac{b_0 z + b_1}{z(z + a_1)}, \quad \begin{cases} a_1 = -e^{-T/\tau}, \\ b_0 = g_0 + g_1(1 - e^{-T/\tau})(1 - d) \quad = \dfrac{1 + \frac{R_p}{R_s}(1 - e^{-T/\tau})(1 - d)}{R_s + R_p}, \\ b_1 = -g_0 e^{-T/\tau} + g_1(1 - e^{-T/\tau})d = \dfrac{-e^{-T/\tau} + \frac{R_p}{R_s}(1 - e^{-T/\tau})d}{R_s + R_p}. \end{cases} \tag{114}$$

$$H(z)=\frac{b_0 z+b_1}{z(z+a_1)},\quad \begin{cases} a_1=-e^{-T/\tau}, & \\ b_0=g_0+g_1(1-e^{-(1-d)T/\tau}) & =\dfrac{1+\frac{R_p}{R_s}(1-e^{-(1-d)T/\tau})}{R_s+R_p}, \\ b_1=-g_0e^{-T/\tau}+g_1(e^{-(1-d)T/\tau}-e^{-T/\tau}) & =\dfrac{-e^{-T/\tau}+\frac{R_p}{R_s}(e^{-(1-d)T/\tau}-e^{-T/\tau})}{R_s+R_p}. \end{cases} \tag{115}$$

This result is also valid for the case without delay, because for $d=0$ the equations (115) and (108) are equal. The zero of this transfer function is

$$\operatorname{zero}(H)=-\frac{b_1}{b_0}=1-\frac{(g_0+g_1)(1-e^{-T/\tau})}{g_0+g_1(1-e^{-T/\tau})(1-d)}=1-\frac{(R_s+R_p)(1-e^{-T/\tau})}{R_s+R_p(1-e^{-T/\tau})(1-d)}\in(-\infty,1), \tag{116}$$

$$\operatorname{zero}(H)=-\frac{b_1}{b_0}=1-\frac{(g_0+g_1)(1-e^{-T/\tau})}{g_0+g_1(1-e^{-(1-d)T/\tau})}=1-\frac{(R_s+R_p)(1-e^{-T/\tau})}{R_s+R_p(1-e^{-(1-d)T/\tau})}\in(-\infty,1), \tag{117}$$

which might be located inside or outside the unit circle. This zero is sufficiently stable for pole-zero cancellation if the delay respects

$$\begin{aligned} \operatorname{zero}(H)\geq-\alpha \quad\Rightarrow\quad d &\leq \frac{1}{1+\alpha}\left(\alpha+\frac{g_0}{g_1}\frac{\alpha+e^{-T/\tau}}{1-e^{-T/\tau}}\right)=\frac{1}{1+\alpha}\left(\alpha+\frac{R_s}{R_p}\frac{\alpha+e^{-T/\tau}}{1-e^{-T/\tau}}\right) \\ &\approx\frac{\alpha}{1+\alpha}+\frac{g_0}{g_1}\left(\frac{\tau}{T}-\frac{1}{1+\alpha}\right)=\frac{\alpha}{1+\alpha}+\frac{R_s}{R_p}\left(\frac{\tau}{T}-\frac{1}{1+\alpha}\right) \\ &=1+\frac{g_0}{g_1}\frac{\tau}{T}-\frac{g_0+g_1}{g_1}\frac{1}{1+\alpha}=1+\frac{R_s}{R_p}\frac{\tau}{T}-\frac{R_s+R_p}{R_p}\frac{1}{1+\alpha}, \end{aligned} \tag{118}$$

$$\begin{aligned} \operatorname{zero}(H)\geq-\alpha \quad\Rightarrow\quad d &\leq 1+\frac{\tau}{T}\ln\left(\frac{g_0+g_1}{g_1}\frac{e^{-T/\tau}+\alpha}{1+\alpha}\right)=1+\frac{\tau}{T}\ln\left(\frac{R_s+R_p}{R_p}\frac{e^{-T/\tau}+\alpha}{1+\alpha}\right) \\ &\approx 1+\frac{g_0}{g_1}\frac{\tau}{T}-\frac{g_0+g_1}{g_1}\frac{1}{1+\alpha}=1+\frac{R_s}{R_p}\frac{\tau}{T}-\frac{R_s+R_p}{R_p}\frac{1}{1+\alpha} \\ &=\frac{\alpha}{1+\alpha}+\frac{g_0}{g_1}\left(\frac{\tau}{T}-\frac{1}{1+\alpha}\right)=\frac{\alpha}{1+\alpha}+\frac{R_s}{R_p}\left(\frac{\tau}{T}-\frac{1}{1+\alpha}\right) \\ &=\frac{\alpha-R_s/R_p}{1+\alpha}+\frac{1}{T}\frac{L}{R_p}\frac{R_s+R_p}{R_p}, \end{aligned} \tag{119}$$

where

$$\alpha=\min(e^{-\omega T},e^{-\frac{\zeta}{\sqrt{1-\zeta^2}}\pi}) \tag{120}$$

to obtain damping of the residual mode—no pole-zero cancellation is perfect—superior to an absolute angular frequency ω and a relative damping factor ζ. In fact, the undesired oscillation, which will be at the Nyquist frequency (alternating positive and negative values), will be damped with a factor α every sample. In practice, this factor should be limited to $\alpha\approx 0.2$ (equivalent to $\omega T=-\ln\alpha\approx 1.6$ and $\zeta=1/\sqrt{1+(\pi/\ln\alpha)^2}\approx 0.45$).

For sampling periods that are small compared to the process time constant, we can approximate the exponential terms as

$$T\ll\tau \quad\Rightarrow\quad e^{-T/\tau}\approx 1-T/\tau, \tag{121}$$

each with a relative error of T/τ. This follows from the Taylor polynomial

$$e^x=\sum_{n=0}^{\infty}\frac{x^n}{n!}=1+x+\frac{x^2}{2}+\frac{x^3}{6}+\cdots \quad \forall x\in\mathbb{R}. \tag{122}$$

Such approximations can be made if their errors are smaller than those of the model parameters.

LHC RST-Controller Synthesis

The load model

$$H(z)=\frac{B}{A}=\frac{b_0 z+b_1}{z(z+a_1)} \tag{123}$$

has two poles and one zero. We will cancel the zero and use a reference model

$$H_m(z) = \frac{B_m}{A_m} = \frac{1}{z} \tag{124}$$

with one pole and no zero, resulting in the factorised polynomials:

$$B^+ = z + b_1/b_0, \tag{125}$$
$$B^- = b_0, \tag{126}$$
$$B'_m = 1/b_0. \tag{127}$$

We will include a double integrator in the controller and no notch filters:

$$R^* = (z-1)^2, \tag{128}$$
$$S^* = 1. \tag{129}$$

The minimum order of the observer polynomial becomes

$$\deg A_o \geq 3. \tag{130}$$

We will use one single and one paired mode

$$A_o = (z + c_1)(z^2 + d_1 z + d_2). \tag{131}$$

With the single mode at frequency ω_1 and the paired mode at natural frequency and damping factor (ω_2, ζ_2), the coefficients are

$$c_1 = e^{-\omega_1 T}, \tag{132}$$
$$d_1 = \begin{cases} -2e^{-\zeta_2\omega_2 T}\cos(\sqrt{1-\zeta_2^2}\omega_2 T) & |\zeta_2| \leq 1 \\ -\left(e^{(-\zeta_2+\sqrt{\zeta_2^2-1})\omega_2 T} + e^{(-\zeta_2-\sqrt{\zeta_2^2-1})\omega_2 T}\right) & |\zeta_2| \geq 1 \end{cases}, \tag{133}$$
$$d_2 = e^{-2\zeta_2\omega_2 T}. \tag{134}$$

$$H(z) = \frac{b_0 z + b_1}{z(z + a_1)} \tag{135}$$
$$H_m(z) = \frac{1}{z} \tag{136}$$
$$B^+ = z + b_1/b_0 \tag{137}$$
$$B^- = b_0 \tag{138}$$
$$B'_m = 1/b_0 \tag{139}$$
$$R^* = (z-1)^2 \tag{140}$$
$$S^* = 1 \tag{141}$$
$$\deg A_o \geq 3 \tag{142}$$
$$A_o = (z + c_1)(z^2 + d_1 z + d_2) \tag{143}$$
$$AR^*R' + B^-S^*S' = A_m A_o \tag{144}$$
$$\deg R' = 0 \tag{145}$$
$$\deg S' = 3 \tag{146}$$
$$\deg R = \deg S = \deg T = 3 \tag{147}$$
$$R' = 1 \tag{148}$$
$$S' = s_0 z^3 + s_1 z^2 + s_2 z + s_3 \tag{149}$$
$$R = z^3 + (b_1/b_0 - 2)z^2 + (1 - 2b_1/b_0)z + b_1/b_0 \tag{150}$$
$$S = s_0 z^3 + s_1 z^2 + s_2 z + s_3 \tag{151}$$
$$T = (z^3 + (c_1 + d_1)z^2 + (c_1 d_1 + d_2)z + c_1 d_2)/b_0 \tag{152}$$

$$z(z+a_1)(z-1)^2 + b_0(s_0z^3 + s_1z^2 + s_2z + s_3) = z(z+c_1)(z^2 + d_1z + d_2) \tag{153}$$

$$a_1 - 2 + b_0s_0 = c_1 + d_1 \tag{154}$$
$$-2a_1 + 1 + b_0s_1 = c_1d_1 + d_2 \tag{155}$$
$$a_1 + b_0s_2 = c_1d_2 \tag{156}$$
$$b_0s_3 = 0 \tag{157}$$

$$r_0 = 1 \tag{158}$$
$$r_1 = (b_1 - 2b_0)/b_0 \tag{159}$$
$$r_2 = (b_0 - 2b_1)/b_0 \tag{160}$$
$$r_3 = b_1/b_0 \tag{161}$$

$$s_0 = (c_1 + d_1 - a_1 + 2)/b_0 \tag{162}$$
$$s_1 = (c_1d_1 + d_2 + 2a_1 - 1)/b_0 \tag{163}$$
$$s_2 = (c_1d_2 - a_1)/b_0 \tag{164}$$
$$s_3 = 0 \tag{165}$$

$$t_0 = 1/b_0 \tag{166}$$
$$t_1 = (c_1 + d_1)/b_0 \tag{167}$$
$$t_2 = (c_1d_1 + d_2)/b_0 \tag{168}$$
$$t_3 = c_1d_2/b_0 \tag{169}$$

16 Conclusion

...

A Natural Frequency and Damping Factor

In the s-domain, the modes with natural frequency ω and damping factor ζ

$$s_{1,2} = \begin{cases} (-\zeta \pm j\sqrt{1-\zeta^2})\omega = -\sigma_0 \pm j\omega_0 & |\zeta| \le 1 \\ (-\zeta \pm \sqrt{\zeta^2 - 1})\omega = -\sigma_{1,2} & |\zeta| \ge 1 \end{cases} \tag{170}$$

are the roots of the polynomial

$$s^2 + 2\zeta\omega s + \omega^2 = \begin{cases} (s+\sigma_0)^2 + \omega_0^2 & |\zeta| \le 1 \\ (s+\sigma_1)(s+\sigma_2) & |\zeta| \ge 1 \end{cases}. \tag{171}$$

The natural frequency and damping factor are related to the modes as

$$\sqrt{s_1s_2} = \omega = \begin{cases} \sqrt{\sigma_0^2 + \omega_0^2} & |\zeta| \le 1 \\ \sqrt{\sigma_1\sigma_2} & |\zeta| \ge 1 \end{cases}, \tag{172}$$

$$\frac{s_1 + s_2}{2} = -\zeta\omega = \begin{cases} -\sigma_0 & |\zeta| \le 1 \\ -\frac{\sigma_1+\sigma_2}{2} & |\zeta| \ge 1 \end{cases}. \tag{173}$$

The modes form a complex conjugate pair for damping factors smaller than one, and two real values otherwise. The modes are unstable for negative damping factors.

In the z-domain, the equivalent modes

$$z_{1,2} = e^{s_{1,2}T} = \begin{cases} e^{-\zeta\omega T} e^{\pm j\sqrt{1-\zeta^2}\omega T} = e^{-\sigma_0 T} e^{\pm j\omega_0 T} & |\zeta| \leq 1 \\ e^{(-\zeta \pm \sqrt{\zeta^2-1})\omega T} = e^{-\sigma_{1,2} T} & |\zeta| \geq 1 \end{cases} \tag{174}$$

are the roots of the polynomial

$$\begin{cases} z^2 - 2e^{-\zeta\omega T}\cos(\sqrt{1-\zeta^2}\omega T)z + e^{-2\zeta\omega T} = (z - e^{-\sigma_0 T}\cos\omega_0 T)^2 + (e^{-\sigma_0 T}\sin\omega_0 T)^2 & |\zeta| \leq 1 \\ z^2 - 2e^{-\zeta\omega T}\cosh(\sqrt{\zeta^2-1}\omega T)z + e^{-2\zeta\omega T} = (z - e^{-\sigma_1 T})(z - e^{-\sigma_2 T}) & |\zeta| \geq 1 \end{cases}. \tag{175}$$

The difference between the two cases arises from $\cos x \in [-1, +1]$ and $\cosh x \in [1, \infty)$ for all $x \in \mathbb{R}$.

In the time domain, such modes correspond to signals of the form

$$u(t) = \begin{cases} \sin(\omega_0 t)e^{-\sigma_0 t} = \sin(\sqrt{1-\zeta^2}\omega t)e^{-\zeta\omega t} & |\zeta| < 1 \\ te^{-\sigma t} = te^{-\omega t} & |\zeta| = 1 \\ e^{-\sigma_1 t} - e^{-\sigma_2 t} = \sinh(\sqrt{\zeta^2-1}\omega t)e^{-\zeta\omega t} & |\zeta| > 1 \end{cases}, \tag{176}$$

with the time being either continuous $t \in \mathbb{R}$ or discrete $t = kT\ \forall k \in \mathbb{Z}$.

B Absolute and Relative Damping

Damping of a mode is related to the speed with which it vanishes in a signal. Absolute damping determines how fast the mode decreases with respect to time, whereas relative damping determines how fast the mode decreases with respect to its own oscillation period.

With ω an absolute angular frequency and ζ a relative damping factor, the region in the complex s-plane that corresponds to modes with superior absolute and relative damping is defined by

$$\Re s \leq -\omega, \tag{177}$$

$$\Re s \leq -\frac{\zeta}{\sqrt{1-\zeta^2}} |\Im s|. \tag{178}$$

Figure 9a shows such a region.

With $z = e^{sT}$, the corresponding region in the complex z-plane is defined by

$$|z| \leq e^{-\omega T}, \tag{179}$$

$$|z| \leq e^{-\frac{\zeta}{\sqrt{1-\zeta^2}}|\arg z|}, \quad \arg z \in [-\pi, +\pi]. \tag{180}$$

Figure 9b shows such a region.

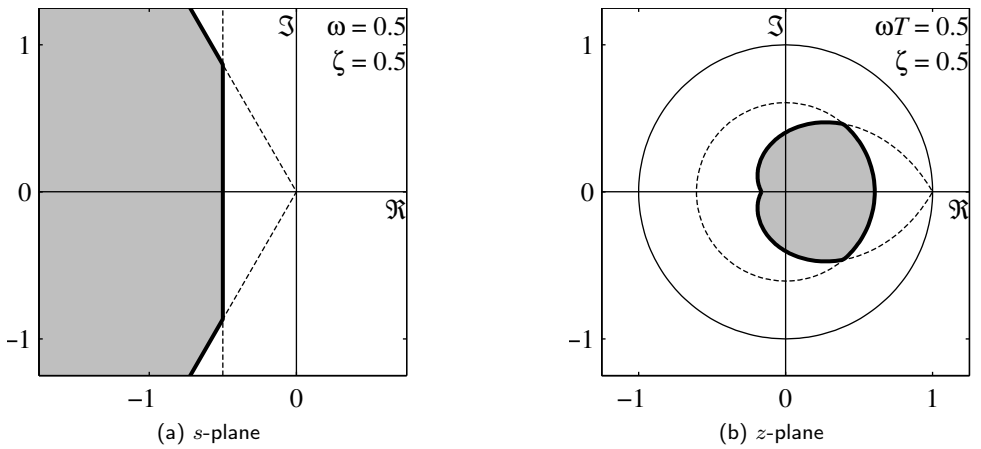

(a) s-plane (b) z-plane

Figure 9: Region of modes with minimum absolute and relative damping.

C Group and Phase Delay

Group delay is a measure of the time delay of the amplitude envelopes of the various sinusoidal components of a signal through a system, and is a function of the frequency of each component. Phase delay is a similar measure of the time delay of the phase of each sinusoidal component [8]. The phase shift ϕ of an LTI-system with transfer function $G(s)$ or $H(z)$ is

$$\phi(\omega) = \begin{cases} \arg G(j\omega) & \text{continuous time} \\ \arg H(e^{j\omega T}) & \text{discrete time} \end{cases} \tag{181}$$

and depends on the frequency ω. The group delay τ_g and phase delay τ_ϕ are related to the phase shift ϕ as

$$\tau_g(\omega) = -\frac{\mathrm{d}\phi(\omega)}{\mathrm{d}\omega} \tag{182}$$

$$\tau_\phi(\omega) = -\frac{\phi(\omega)}{\omega} \tag{183}$$

and also depend on the frequency ω [8]. In discrete time, the group delay and phase delay are proportional to the sampling period.

In a linear-phase system (with non-inverting gain), both τ_g and τ_ϕ are constant and equal to the same overall time delay of the system, and the unwrapped phase shift ϕ is negative with its magnitude increasing linearly with the frequency ω [8]. A linear-phase system with unit gain is called a pure delay.

For a transfer function

$$\begin{cases} G(s) = k\frac{\prod_i s-z_i}{\prod_j s-p_i}e^{-s\tau} & \text{continuous time} \\ H(z) = k\frac{\prod_i z-z_i}{\prod_i z-p_i}z^{-\ell} & \text{discrete time} \end{cases} \tag{184}$$

with gain k, zeros z_i, poles p_i and a pure delay τ respectively ℓT, the group delay equals

$$\tau_g(\omega) = \begin{cases} \tau + \sum_i \Re\frac{1}{j\omega-p_i} - \sum_i \Re\frac{1}{j\omega-z_i} & \text{continuous time} \\ T\left[\ell + \sum_i \Re\frac{e^{j\omega T}}{e^{j\omega T}-p_i} - \sum_i \Re\frac{e^{j\omega T}}{e^{j\omega T}-z_i}\right] & \text{discrete time} \end{cases}. \tag{185}$$

References

[1] R. C. Dorf, *Modern Control Systems*, 5th ed., ser. Addison-Wesley Series in Electrical and Computer Engineering: Control Engineering. Reading, Mass. (USA): Addison-Wesley, 1989.

[2] K. J. Åström and B. Wittenmark, *Computer-Controlled Systems: Theory and Design*, 2nd ed., ser. Prentice Hall Information and System Sciences Series, T. Kailath, Ed. Englewood Cliffs, N.J. (USA): Prentice-Hall, 1990.

[3] R. Longchamp, *Commande numérique de systèmes dynamiques*, 1st ed. Lausanne (CH): Presses Polytechniques et Universitaires Romandes, 1995.

[4] I. D. Landau, *Identification et commande des systèmes*, 2nd ed., ser. Traité des Nouvelles Technologies, série Automatique. Paris (F): Hermès, 1993.

[5] H. Bühler, "Théorie," in *Réglage de systèmes d'électronique de puissance*, 1st ed., ser. Collection Électricité. Lausanne (CH): Presses Polytechniques et Universitaires Romandes, 1997, vol. 1.

[6] F. Bordry and H. Thiesen, "RST digital algorithm for controlling the LHC magnet current," European Organization for Nuclear Research, Genève (CH), Tech. Rep. CERN LHC-258, Dec. 1998.

[7] A. Papoulis, *Circuits and Systems: A Modern Approach*, 1st ed., ser. HRW Series in Electrical and Computer Engineering, M. E. van Valkenburg, Ed. Fort Worth, Tex. (USA): Holt, Rinehart and Winston, 1980.

[8] Wikipedia. Internet encyclopedia. Wikimedia Foundation. San Francisco, Calif. (USA). Available: http://www.wikipedia.org

[9] D. Garcia, A. Karimi, and R. Longchamp, "Robust PID controller tuning with specification on modulus margin," in *Proceedings of the American Control Conference (ACC)*, vol. 4, Jun. 2004, pp. 3297–3302.

[10] S. Sterpu, "Robustness margins in electric power systems," in *Proceedings of the IEEE Power and Energy Society General Meeting (PES)*, Jul. 2008.

[11] H. Thiesen, "Étude simplifiée des boucles de courant R-S-T pour les convertisseurs de puissance du LHC," European Organization for Nuclear Research, Genève (CH), Tech. Rep. CERN EDMS-686163, Dec. 2005.

[12] H. Thiesen, "Modélisation des chaînes d'aimants supraconducteurs avec résistances d'amortissement," European Organization for Nuclear Research, Genève (CH), Tech. Rep. CERN EDMS-686170, Dec. 2005.